from a dictionary of functions. These waveforms are chosen in order to best match the signal structures (Mallat et al., 1993; Wang, 2006). The disadvantage of MPD is lateral discontinuity and computational complexity. Recently, a lot of work has been done on spectral decomposition using synchrosqueezing transform (Chen et al., 2014 and Wang et al., 2014) and S transform (Huang et al., 2015 and Liu et al., 2017). Followed by spectral decomposition, spectral balancing is done irrespective of the spectral decomposition technique used. In this, the amplitude of the spectral frequencies are enhanced where it is low. Thus, making it perfectly balanced over all the frequencies (Chopra et al., 2016).

The following sections explain the detailed algorithm thoroughly. The proposed workflow is shown in Fig. 1. At first, the dip is estimation using complex trace analysis which is further enhanced using the Gaussian/Laplacian pyramid. The estimated dip is used in filtering the seismic data using the dip steered median filter. Followed by this, continuous wavelet transform is applied on the dip steered median filtered volume using various wavelets. Followed by this, spectral balancing is employed. Finally, the paper is concluded in the final section.

Dip Estimation

Dip attribute determines the best fit line in 2D seismic data or the best-fit plane in 3D seismic volume for every trace between the neighboring traces on a horizon. Taner et al., 1979 proposed a dip estimation technique using complex trace analysis.

Further, the weighted average of the dip is calculated to obtain the smoother seismic section (Barnes 2000). But complex trace analysis suffers from waveform interference and instantaneous frequency can fall outside the seismic bandwidth resulting in negative values. Hence, to enhance the dip attribute, the Gaussian/Laplacian pyramid approach is employed to reduce the noise and preserve the edges in the data (Mahadik R. et al., 2019). Further, dip steered median filter (DSMF) is applied to the inline section which removes the random noises and enhances lateral continuity of the reflections in the seismic data (Francelino 2013). This additionally provides an enhanced signal to noise ratio.
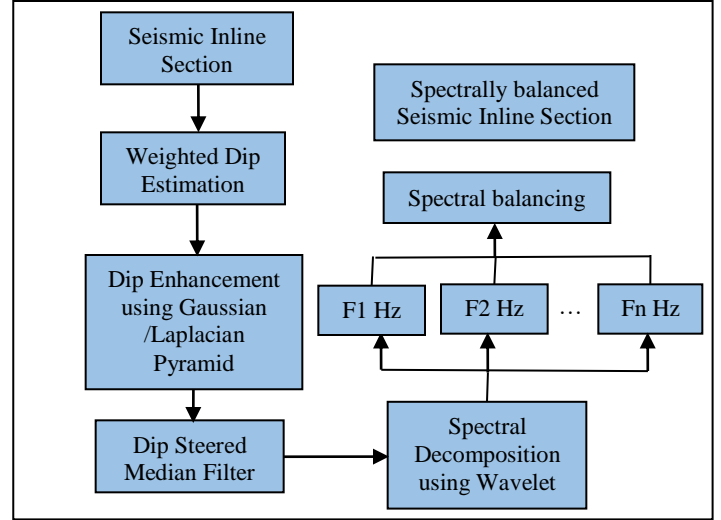

Figure 1: Proposed Workflow.

Spectral Decomposition

Spectral decomposition decomposes the time-dependent seismic trace into time-dependent frequency bands. Improved spectral decomposition in TF space is provided by the sliding window i.e., short-time Fourier transform. But this method suffers from the TF resolution limitation since the window length is predefined. Time resolution is poor in case of short window length and frequency resolution is poor in long window length. This issue is resolved in CWT which uses variable window length and hence increases the temporal and spectral resolution. The continuous wavelet transform is given as:

$$W_{(a,b)} = \frac{1}{\sqrt{a}} \int \psi^* \left(\frac{t-b}{a} \right) f(t) dt \qquad (1)$$

where a is a scaling parameter, b is a translation parameter, ψ is the mother wavelet, $f(t)$ is the signal, and $W(a,b)$ is the CWT scale decomposition. Complex wavelets such as Morlet, Ricker, Shannon and DOG wavelets are used in the complex wavelet transform in which the real and imaginary (i.e. phase rotated) wavelets are simply convolved with the input seismic trace to form complex voice components. Voice components introduced by Goupillaud et al., 1984 are the function of spectral magnitude and the phase. It is given as:

$$v(t,f) = m(t,f) \exp \left[-j\phi(t,f) \right] \qquad (2)$$

Fault Interpretation using Spectral Decomposition and Spectral Balancing

Spectral Balancing

The main objective of spectral balancing is to enhance the low-resolution frequency components of spectral decomposition to obtain a perfectly balanced resolution. If the seismic data is spectrally balanced or in simple words, if the frequency bandwidth is extended, the resulting data can have a higher vertical and lateral resolution. The power spectrum of the data is given in Figure 1. It can be seen that the normalized power deteriorates after 30 Hz. This leads to using few frequency components and some spectral information may be missing in the low-frequency components such as fault and fractures. For better fault interpretation, it is highly likely to balance the data spectrally.
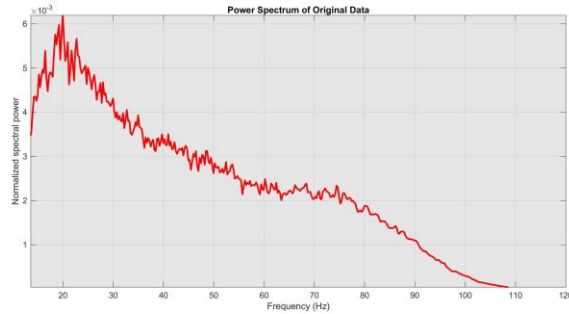

Figure 2: Normalized power spectrum of a KG basin seismic volume before spectral balancing.

The spectral balancing magnitude is given as (Fatima *et al.*, 2010, Chopra *et al.*, 2016):

$$m_j^{bal}(t,f) = \left[\frac{P_{peak}(t)}{\alpha P_{peak}(t) + P_{avg}(t,f)} \right]^{\frac{1}{2}} m(t,f) \quad (3)$$

where $P_{avg}(t,f)$ is the smoothed average power spectrum obtained by averaging the power of spectral magnitude given by $P(t,f) = m(t,f)^2$ overall the traces in the seismic volume in a given predefined time window. $P_{peak}(t)$ is the peak of the average spectrum. α is the prewhitening parameter which is 0.04 in normal cases and can be taken as 0.01 in larger surveys to further broaden the spectrum. Each frequency band is equalized by its scaling function which depends upon the amplitude levels in this band. All these scaled frequency bands together are added to obtain the balanced sections. Some applications allow a percentage of the input data to be added back to improve the results. Rigorous testing needs to be performed on the data to enhance the frequency spectra within sensible bandwidth.
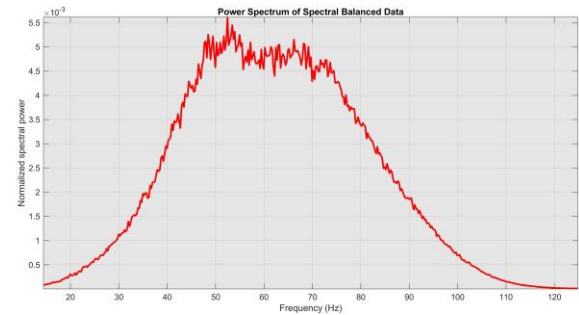

Figure 3: Normalized power spectrum of a KG basin seismic volume after spectral balancing.

Experimental Results

For this study, the input data is a 3D seismic processed post-stack data volume, located in the offshore K.G. Basin, licensed by GEOPIC, ONGC, Dehradun. The inline range is from 1982 to 4517, the crossline range is from 8800 to 14000 with a step size of 2. The data is recorded for 4 seconds with the sampling interval of 4ms. The original seismic section with inline 3000 is as shown in Fig. 4.

Spectral balancing of frequencies from 5 to 90 Hz provided good results in improving the resolution without increasing noise. The spectral balancing of frequencies beyond 90 Hz produces more noises. The power spectrum of seismic data after spectral balancing is depicted in Fig. 3.

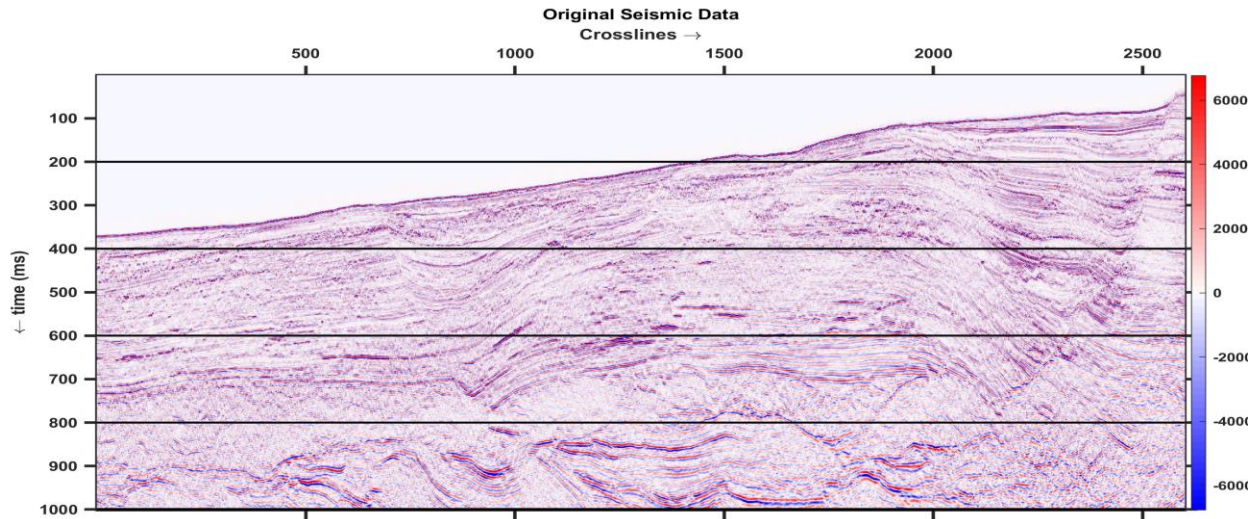**Fault Interpretation using Spectral Decomposition and Spectral Balancing**

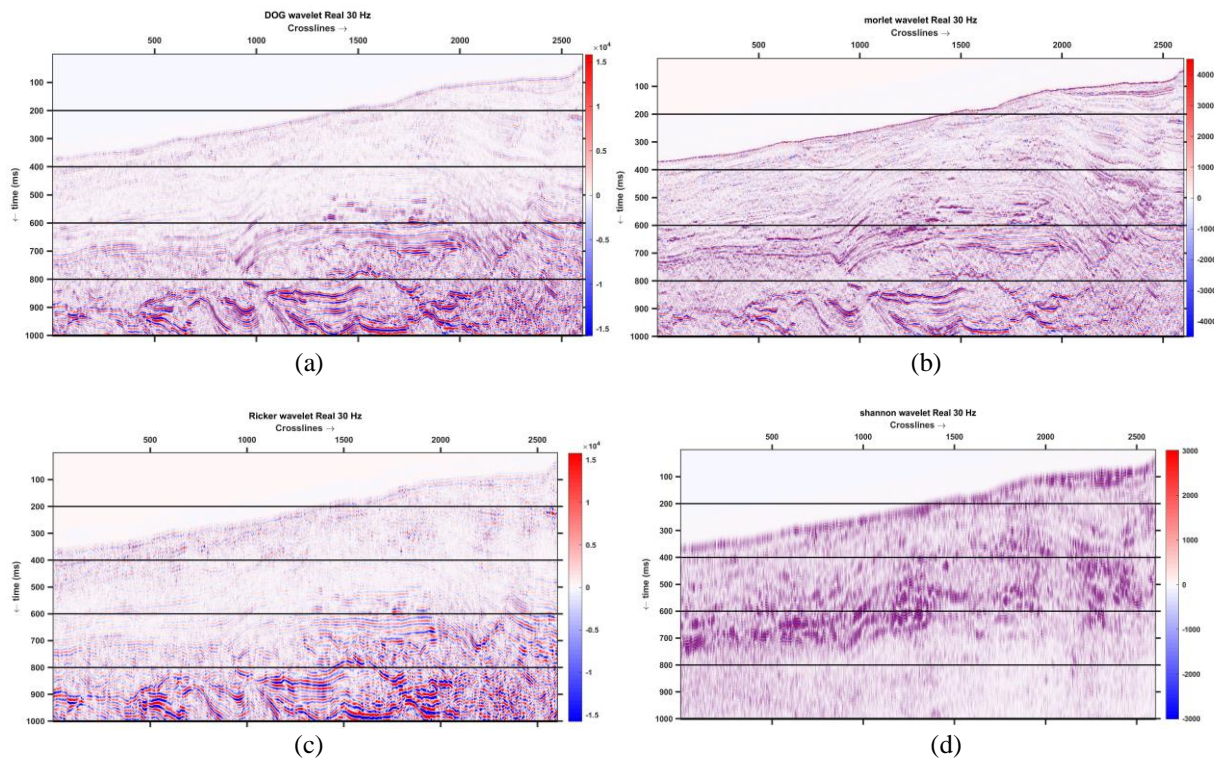Figure 4: Original inline seismic section (Inline number: 3000)

Figure 5: 30 Hz spectral decomposition component of an inline section using a) DOG wavelet; b) Morlet wavelet; c) Ricker wavelet; d) Shannon Wavelet
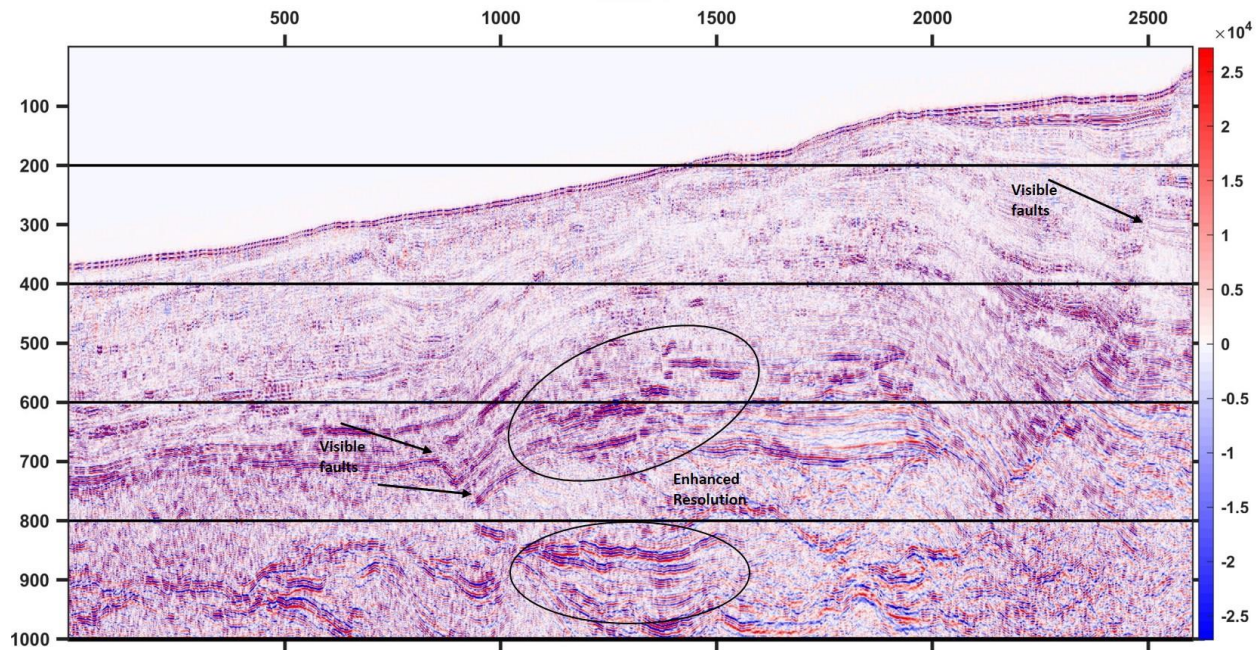
Figure 5: Enhanced seismic inline section after spectral balancing with annotations.

After generating the complex wavelets such as DOG, Morlet, Ricker and Shannon, of 30 Hz center frequency, it is convolved with seismic traces and the 30Hz spectral component is generated. The spectral component of DOG, Morlet, Ricker and Shannon wavelets are illustrated in Fig. 4. From the figure, it is evident that the Morlet wavelet shows better results than others. Other wavelets distort the section and invite discontinuities. Fig. 5 shows an enhanced seismic inline section after spectral balancing. The region contained in ellipse shows the enhanced resolution of the seismic section and the arrows show the perceptible fault visibility.

Conclusions

Spectral decomposition converts the signal into the TF domain, where the time and frequency can be analyzed simultaneously. To obtain TF analysis, CWT is employed using Shannon, Morlet, DOG and Ricker wavelets. Among these, the Morlet wavelet gives better results than others. But the spectral distribution is not perfectly balanced and high-frequency components have a low amplitude. In order to interpret faults which are usually high frequency components, spectral balancing is used to stretch the bandwidth and enhance the amplitude where the resolution was poor. This evenly balances the spectrum and faults are not easily visible in the seismic data. This helps geologists and geophysicists study and interprets the subtle and minor faults in a seismic volume. In future, we aim to delineate the faults automatically using machine learning algorithms on the spectrally balanced seismic volume.

References

Barnes, A.E., 2000. Weighted average seismic attributesAverage Seismic Attributes. Geophysics, 65(1), pp.275-285.

Castagna, J.P. and Sun, S., 2006. Comparison of spectral decomposition methods. First break, 24(3).

Chakraborty, A. and Okaya, D., 1995. Frequency-time decomposition of seismic data using wavelet-based methods. Geophysics, 60(6), pp.1906-1916.

Fault Interpretation using Spectral Decomposition and Spectral Balancing

Chen, Y., Liu, T., Chen, X., Li, J. and Wang, E., 2014. Time-frequency analysis of seismic data using synchrosqueezing wavelet transform. In SEG Technical Program Expanded Abstracts 2014 (pp. 1589-1593). Society of Exploration Geophysicists.

Chopra, S. and Marfurt, K.J., 2015a. Choice of mother wavelets in CWT spectral decomposition. In SEG Technical Program Expanded Abstracts 2015 (pp. 2957-2961). Society of Exploration Geophysicists.

Chopra, S. and Marfurt, K.J., 2015b. Enhancing interpretability of seismic data with spectral decomposition phase components. In SEG Technical Program Expanded Abstracts 2015 (pp. 1976-1980). Society of Exploration Geophysicists.

Chopra, S. and Marfurt, K.J., 2016. Spectral decomposition and spectral balancing of seismic data. The Leading Edge, 35(2), pp.176-179.

Fatima, M., Kumar, L., Bhattacharjee, R.K., Rao, P.H. and Sinha, D.P., 2010, February. Improving Resolution with Spectral Balancing-A Case study. In 8th Biennial International Conference & Exposition on Petroleum Geophysics, Hyderabad, India (Vol. 13).

Francelino, A.V.M. and Antunes, A.F., 2013. Applying filters and seismic attributes for enhancing faults in the 3D seismic survey of Alto De Siririzinho (Sergipe-Alagoas Basin, northeast Brazil). Revista Brasileira de Geofisica, 31(1), pp.109-123.

Goupillaud, P., Grossmann, A. and Morlet, J., 1984. Cycle-octave and related transforms in seismic signal analysis. Geoexploration, 23(1), pp.85-102.

Huang, Z.L., Zhang, J., Zhao, T.H. and Sun, Y., 2015. Synchrosqueezing S-transform and its application in seismic spectral decomposition. IEEE Transactions on Geoscience and Remote Sensing, 54(2), pp.817-825.

Kola, V.R., Singh, N., Desai, A., Chacko, S. and Mohapatra, P., Interpretation of Subtle Channel-Fan system in Dharvi Dungar Formation of Barmer Basin, India using Calibrated Spectral Decomposition Data.

Liu, N., Gao, J., Zhang, B., Li, F. and Wang, Q., 2017. Time–frequency analysis of seismic data using a three parameters S transform. IEEE Geoscience and Remote Sensing Letters, 15(1), pp.142-146.

Mahadik, R., Routray, A., 2019. Fault Detection and Optimization in Seismic Dataset using Multiscale Fusion of a Geometric Attribute. In IECON 45th Annual Conference of the IEEE Industrial Electronics Society. IEEE. (Forthcoming)

Mallat, S.G. and Zhang, Z., 1993. Matching pursuits with time-frequency dictionaries. IEEE Transactions on signal processing, 41(12), pp.3397-3415.

Sinha, S., Routh, P.S., Anno, P.D. and Castagna, J.P., 2005. Spectral decomposition of seismic data with continuous-wavelet transform. Geophysics, 70(6), pp.P19-P25.

Taner, M.T., Koehler, F. and Sheriff, R.E., 1979. Complex seismic trace analysis. Geophysics, 44(6), pp.1041-1063.

Wang, P., Gao, J. and Wang, Z., 2014. Time-frequency analysis of seismic data using synchrosqueezing transform. IEEE Geoscience and Remote Sensing Letters, 11(12), pp.2042-2044.

Wang, Y., 2006. Seismic time-frequency spectral decomposition by matching pursuit. Geophysics, 72(1), pp.V13-V20.

Acknowledgments